NISTIR 8234

Preparation of Cylindrical Tensile Specimens for Simultaneous Mechanical Testing and X-ray Computed Tomography

Felix H. Kim
Shawn P. Moylan
Edward J. Garboczi

This publication is available free of charge from:
https://doi.org/10.6028/NIST.IR.8234

National Institute of Standards and Technology
U.S. Department of Commerce

NISTIR 8234

Preparation of Cylindrical Tensile Specimens for Simultaneous Mechanical Testing and X-ray Computed Tomography

Felix H. Kim
Shawn P. Moylan
Engineering Laboratory

Edward J. Garboczi
Material Measurement Laboratory

This publication is available free of charge from:
https://doi.org/10.6028/NIST.IR.8234

March 2019

U.S. Department of Commerce
Wilbur L. Ross, Jr., Secretary

National Institute of Standards and Technology
Walter Copan, NIST Director and Under Secretary of Commerce for Standards and Technology

Abstract

Cylindrical tensile specimens were designed and prepared for simultaneous mechanical testing and X-ray computed tomography (XCT). Laser powder bed fusion-based metal additive manufacturing was used to produce tensile specimens to near-net shapes. Natural and simulated defects were embedded in the tensile specimen using the additive manufacturing process. Conventional machining was used to refine the shape of the tensile specimens to their final shapes with low surface roughness. The process of developing a cylindrical tensile specimen is described and recommendations for future builds are provided. An XCT-based dimensional measurement technique to inspect the part quality is introduced and described.

Key words

Additive manufacturing; Cylindrical tensile specimen; Defect embedment; X-ray computed tomography.

Table of Contents

List of Tables

List of Figures

1. Introduction

Cylindrical tensile specimens were designed and prepared for simultaneous mechanical testing with X-ray computed tomography (XCT). The purpose of the experiment is to study the failure mechanism due to both simulated and natural defects of Additive Manufacturing (AM). A load frame (CT-5000) specifically designed for the mechanical testing with XCT was acquired from Deben UK Ltd[1]. The rough shape of the tensile specimens was built using laser powder bed fusion-based metal Additive Manufacturing (AM). Conventional machining refined each specimen to its final shape. Different initial shapes were built with AM to understand the effect of initial shape on machinability. Some of the specimens contained embedded internal defects by either changing the AM processing parameter or by designing features within the specimen. The designing, fabrication, machining, and post-processing (e.g., heat treatment) steps were documented for future references. A standard procedure for preparing a mechanical test specimen has not been established for additively manufactured metal components. The developed procedure may be applicable to different types and sizes of mechanical test specimens produced with metal AM.

2. Specimen Geometry

The cylindrical specimen geometry was chosen to reduce the possible occurrence of imaging artifacts in XCT scans. The ASTM E8/E8M standard [1] was used as a reference for developing a design for the cylindrical tensile specimens. ASTM recommended the smallest cylindrical specimen to have a diameter of 2.5 mm and a gauge length of 10 mm (for the case with the gauge length four times the diameter). The reported tensile strength of the material (17-4 stainless steel) and the load capacity (5 kN) of the load frame were also considered when determining the gauge diameter of the specimen. The yield strength and ultimate tensile strength for the material were reported by the vendor [2], as shown in Table 1. For a 2.5 mm diameter cross section, the ultimate load was expected to be less than the load capacity (5 kN) of the load frame. Defects intentionally placed in the specimen are expected to reduce the tensile strength. After initial tests (AM Build 1), the diameter of cylindrical tensile specimens were further reduced to 2.25 mm (AM Build 2) to sufficiently achieve a specimen failure within the 5 kN load capacity. The minor deviations in specimen geometry from the standard design were considered acceptable as the purpose of the experiment is to study the failure mechanism rather than measuring standard material properties. The targeted spatial resolution and X-ray penetration capacity were also considered for the 2.5 mm-diameter specimen, as shown in Fig. 1. The X-ray attenuation coefficient of a material is the amount of X-ray being scattered or absorbed while the X-ray travels through a material. This coefficient is used in the Beer-Lambert law, and it was estimated from the National Institute of Standards and Technology (NIST) XCOM data [3] and the material density. If the full gauge width fits in the field of view (FOV) for a 1000 × 1000 pixels detector, approximately 2.5 μm voxel size can be achieved in the XCT image. About 20 % to 40 % X-ray transmission is expected for 160 kV of X-ray source voltage depending on the filter material and thickness, which is an acceptable X-ray transmission level.

[1] Certain commercial equipment, instruments, or materials are identified in this paper in order to specify the experimental procedure adequately. Such identification is not intended to imply recommendation or endorsement by the National Institute of Standards and Technology, nor is it intended to imply that the materials or equipment identified are necessarily the best available for the purpose.

Table 1. Upper yield strength, ultimate strength of 17-4 stainless steel (provided by the AM machine vendor), and expected yield and ultimate load for the chosen specimen design (The horizontal build direction is parallel to AM layers, and the vertical direction is perpendicular to AM layers)

	As-Built		Stress Relieved	
AM Build Direction	Horizontal	Vertical	Horizontal	Vertical
Upper Yield Strength (MPa)	645	630	634	595
Ultimate Strength (MPa)	930	960	1100	980
Diameter (mm)	2.5	2.5	2.5	2.5
Cross-sectional Area (mm^2)	4.91	4.91	4.91	4.91
Expected Yield Load (N)	3166	3093	3112	2921
Expected Ultimate Load (N)	4565	4712	5400	4811

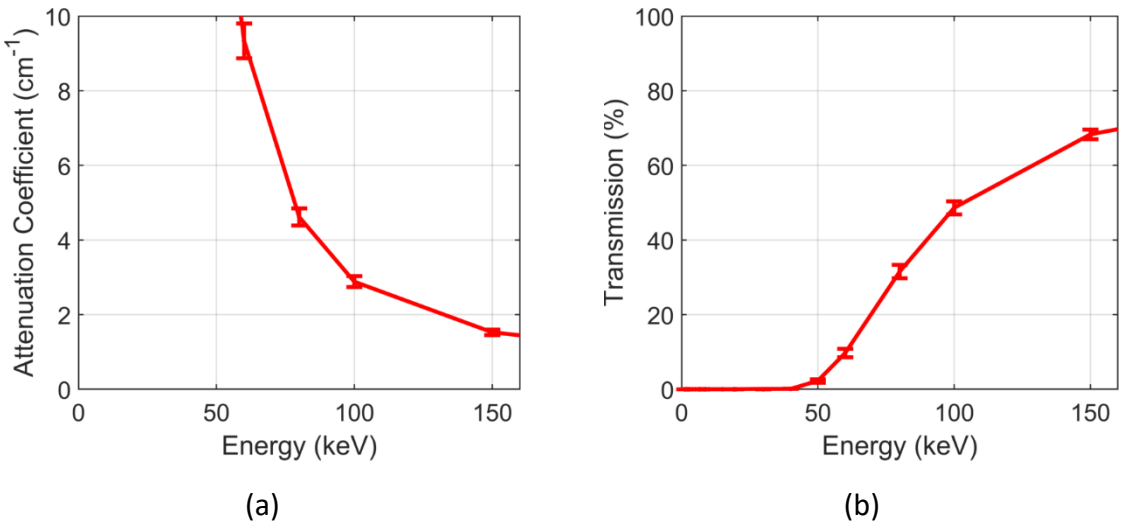

Fig. 1. (a) X-ray attenuation coefficient and (b) transmission of 17-4 stainless steel for 2.5 mm diameter

3. Load Frame and Grips

The tension/compression load frame is shown in Fig. 2. It has a load cell capacity of 5 kN, and up to 10 mm of cross head travel distance for a tensile test. The system is designed to be installed on various types of XCT systems. The cover has a glassy carbon window that is transparent to X-rays. The specimen is loaded between the vendor-provided grips.

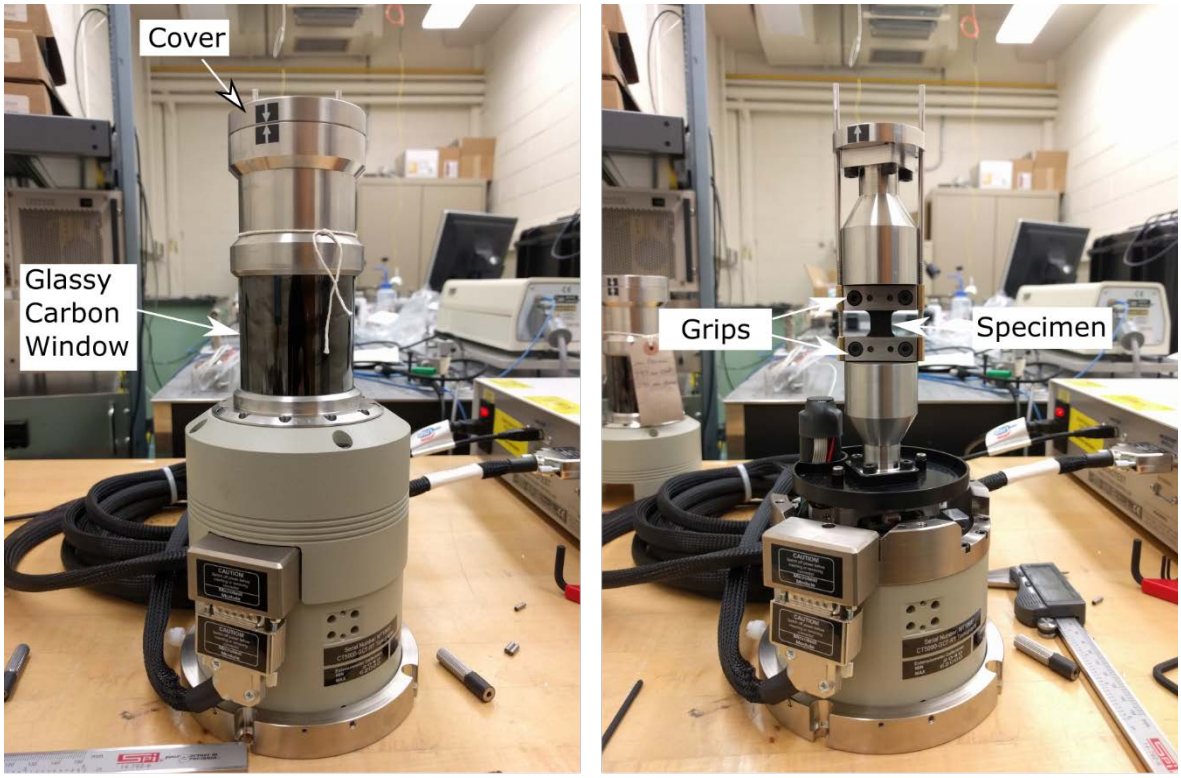

Fig. 2. Load frame for *in situ* mechanical test

The grips to hold the cylindrical specimens are made from a gauge plate, which is a grade 01 tool steel. The hardness of this type of steel is generally higher than 55 HRC depending on the tempering temperature. The grips incorporate grooves with a 1 mm pitch. The angle of the groove tip is 90°. Two sets of grips with different groove sizes were received: One has the major diameter of 5.5 mm (minor diameter: 4.5 mm), and the other has the major diameter of 5 mm (minor diameter 4 mm). The grip sections are 12 mm in length for both top and bottom. The minimum distance between the bottom and top grips is 10 mm. The distance between the bottom and top grips is defined as the gauge length in this paper. The maximum travel distance of the moving head of the load frame is 10 mm. If the sample gauge length increases, then the head travel distance reduces accordingly. For example, the head travel distance is 7 mm for a sample with gauge length of 13 mm. An example assembly is shown in Fig. 3. The thinner grip is called the lower grip, and the thicker one is called the upper grip. There are two of each to hold the top and bottom of the specimen.

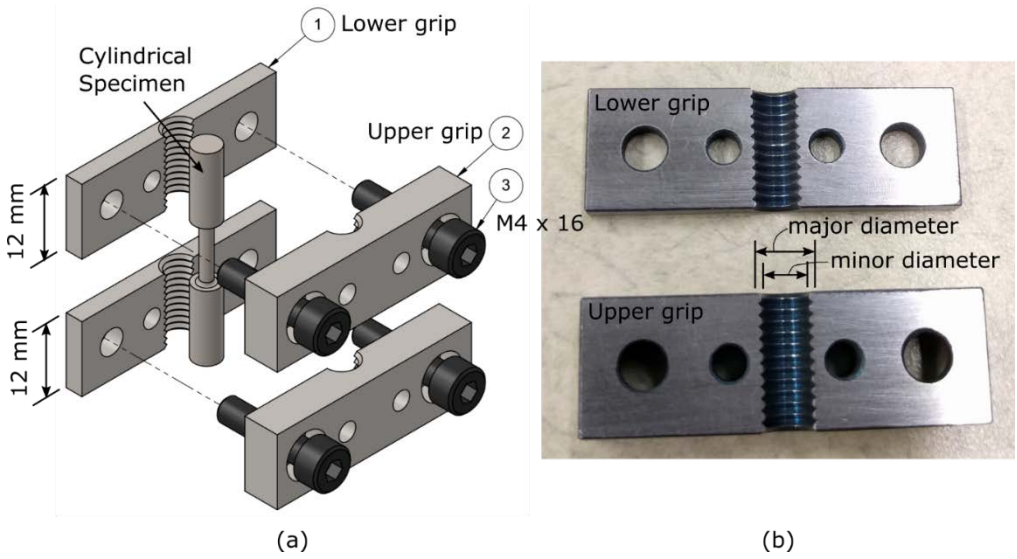

Fig. 3. (a) Design assembly of cylindrical specimen grips with grooves and (b) picture of the grips

4. AM Build 1

A test AM build was performed to understand the buildability and machinability of the small tensile specimens. The cylindrical specimens were built vertically. Protective tubes were built around the samples to prevent the re-coater arm from knocking the sample off from the build plate. The build plate is shown in Fig. 4. The cylindrical specimens were removed from the build plate using electro discharge machining (EDM), and then a residual stress-relief heat treatment was applied. As the samples were built vertically, part deformation due to residual stress was not observed. It is generally recommended to perform a residual stress-relief heat treatment prior to removing parts from the build plate, which was done for the AM Build 2. Based on the recommendation of the vendor [2], the heat treatment process was performed at 650 ^{o}C for 1 h followed by air cooling.

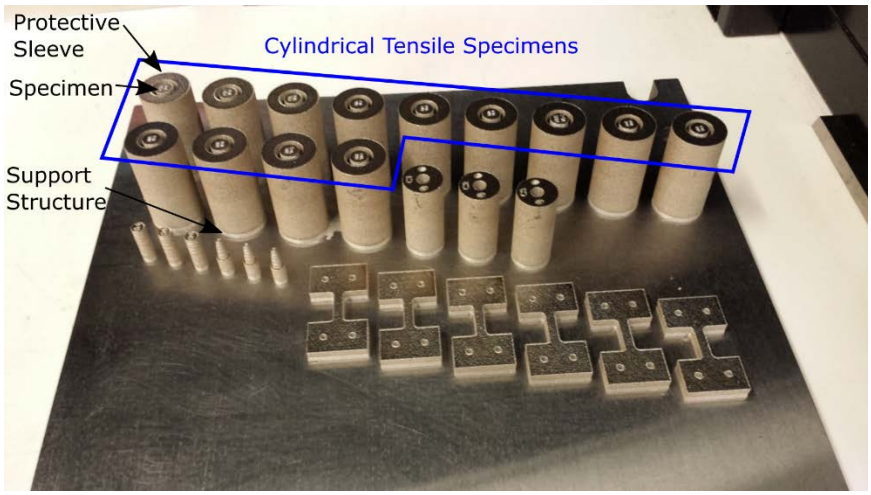

Fig. 4. Build plate of a test build with cylindrical tensile specimens

The as-built AM surfaces are generally rough, which can be stress concentrators and can potentially yield locally, thus act as fracture initiation points. The rough surfaces need to be machined. Three different designs were considered for building the cylindrical specimens and for evaluating post-machinability: cylinder (Design 1), hybrid (Design 2), and near-net shape (Design 3). The three designs and the final shape are shown in Fig. 5. The cylinder shape was 6.5 mm in diameter and approximately 37 mm in height. The hybrid design was built 1 mm larger in diameter than the final shape, but it does not have grooved grip sections. The near-net shape was similar to the hybrid design including the grooved sections. As there are reduced diameter gauge sections, the hybrid and near-net shape designs had support structures (e.g., lattice structures) built around the gauge sections. A manual lathe was used to fabricate the specimens to the final shape. One of the purposes of the study was to determine the machinability of initial designs. According to the machinist, the different initial shapes did not affect machining using a manual lathe in terms of time and effort. Therefore, Design 2 was selected going forward with this study.

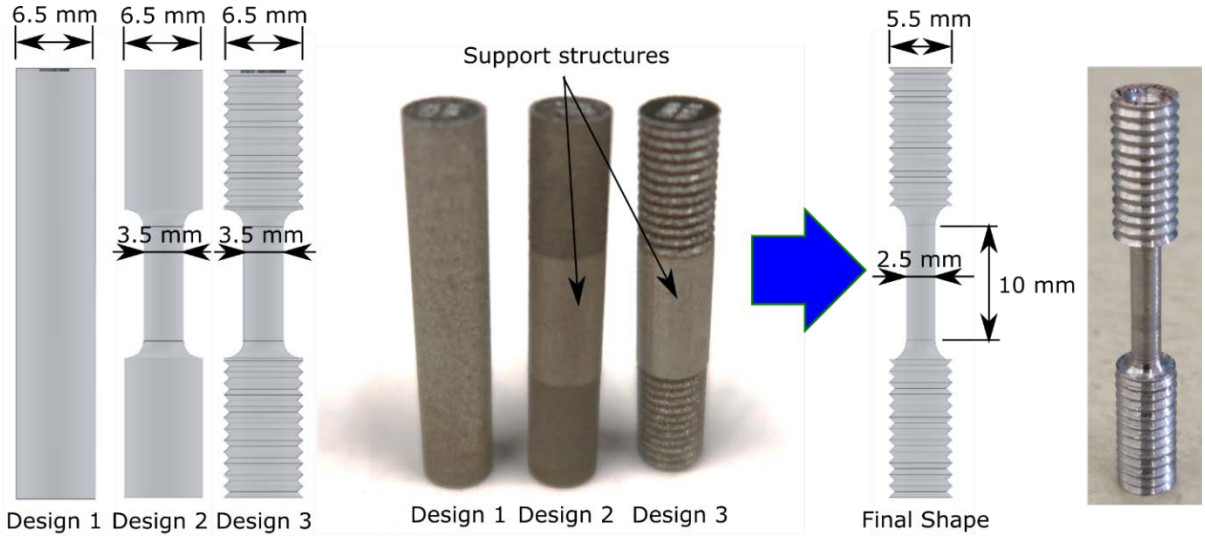

Fig. 5. Machining process for different initial AM-produced geometries

These specimens, however, were built prior to receiving the load frame specimen grips. The machined specimen did not fit into the grips. XCT-based inspections were applied for both the grips and a specimen since the technique provides a rather quick three-dimensional inspection result. The North Star Imaging (NSI) CXMM 50 XCT system on loan to the Physical Measurement Laboratory (PML) Dimensional Metrology Group of NIST was used for the inspection of a specimen and the grips. The voxel size was determined to be 19.8 µm by a calibration object. The acquisition parameters are shown in Table 2. Separate XCT scans were acquired for a tensile specimen, the lower grip, and the upper grip. About 10 min acquisition time was used per scan. Based on the VDI/VDE 2630-1.3 standard [4], the Maximum Permissible Error (MPE) for the point-to-point length measurements was stated by the vendor as (3.5 + L/50) [µm], where L is up to the maximum dimension of the sample in units of mm (The equation already accounts for the unit of L, and only the numeric value of L is used). An MPE is an envelope of maximum error for various point-to-point length

measurements found for a reference object, and this value is reported by the vendor for the XCT system. In this case, the MPE was found to be about 4.3 µm for point-to-point length measurement. The MPE incorporates uncertainty related to systematic error, repeatability of measurements, and uncertainty of the XCT analysis software algorithm. The error for diameter measurement based on least-squares fitting is expected to be smaller than the point-to-point length measurement MPE.

Table 2. XCT acquisition parameters

Parameter	Value
Voltage (kV)	200
Current (µA)	110
Target material	Tungsten
Filter	Copper
Source-to-Detector Distance (mm)	590.9
Source-to-Object Distance (mm)	92.3
Magnification	6.4
Flat panel detector pixel size (µm)	127
Voxel Size (µm)	19.8
Number of Projection	750
Frames per Projection	1
Exposure Time (s)	0.5
Beam hardening Correction	No

VGStudioMax 3.0 was used to read the acquired XCT data and perform dimensional measurements. An appropriate surface was determined based on a local sub-voxel surface determination algorithm [5], and a circle was fit to the groove to determine the size of the groove based on Gaussian (least squares) fit. Example diameter measurements based on circle fits are shown in Fig. 6, and example measurements are compared in Table 3. While the major diameter of the tensile specimen was close to the nominal value, the minor diameter was more than 500 µm larger than the nominal value. The deviation was mainly due to the machining limit at the tip of the groove. Based on the inspection results, the loading system and cylindrical specimen grips were accepted from the vendor during the procurement process, and the cylindrical tensile specimens were returned to the machine shop for further machining.

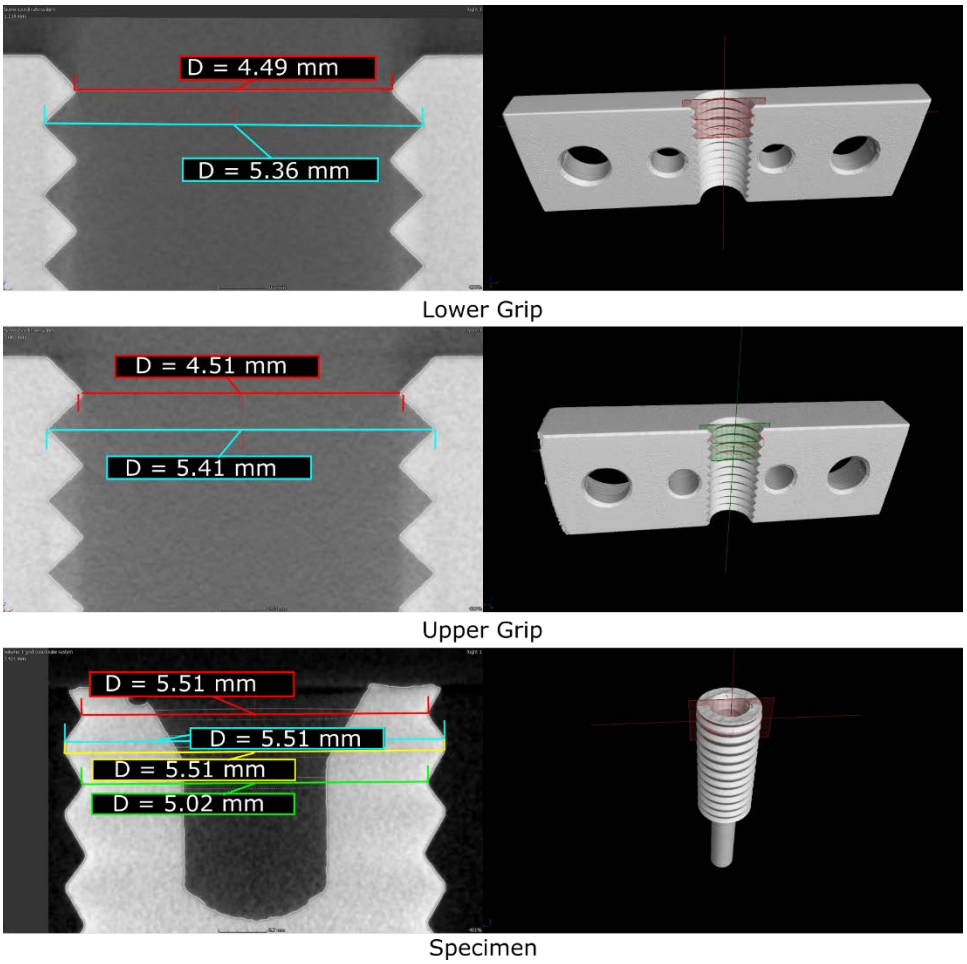

Fig. 6. Example diameter measurement results

Table 3. Comparison of XCT-based inspection measurements of major and minor diameters of grooves

	Major Diameter (mm)	Minor Diameter (mm)
Nominal Design	5.5	4.5
Tensile Specimen	5.51	5.03
Lower Grip	5.36	4.50
Upper Grip	5.41	4.51

5. AM Build 2

A second set of specimens was developed in the hybrid design (design 2) shape shown in Fig. 5, which included some intentional defects built in the middle. Recycled 17-4 Stainless steel powders (GP1) were used. The specimens contain naturally occuring or simulated defects in the middle of the gauge section. The naturally occurring defects were produced by changing AM processing parameters. Simulated defects were designed in Computer-Aided

Design (CAD). The design of the final shape was also slightly modified from the previous design.

The specimens with naturally occurring defects (N0-N4) were produced by changing AM processing parameters in the center of the gauge (1.5 mm dia. × 1.5 mm height cylinder). The AM processing parameters are shown in Table 4. The N0 parameter set is the default parameter of the system, and is used for rest of the specimen volume. The parameters were changed similar to what was done in a recent work of the authors [6].

Table 4. AM processing parameters for specimen N0 – N4

Specimen	Laser power (W)	Scan speed (mm/s)	Hatch spacing (mm)	Energy Density (10^9 J/m^3)
N0 (default)	195	1000	0.1	97.5
N1	195	2000	0.1	48.8
N2	195	1000	0.2	48.8
N3	195	4000	0.1	24.4
N4	195	1000	0.4	24.4

Different types of simulated defects were embedded. The initial trial of embedding simulated defects was described in an earlier work [7]. The work showed that the top surfaces of spheres were not built properly, and spheres smaller than 200 µm were not built at all. The feature sizes are generally around 1 mm. The embedded defects are two types of sphere defects (S1 and S2), three types of ellipsoid defects (E1, E2, and E3), two types of annular crack (AC1 and AC2), three types of octahedron (O1, O2, and O3), and a crack defect (C). The initial build geometry and embedded defects are shown in Fig. 7. Five specimens of each type were fabricated. The build plate is shown in Fig. 8.

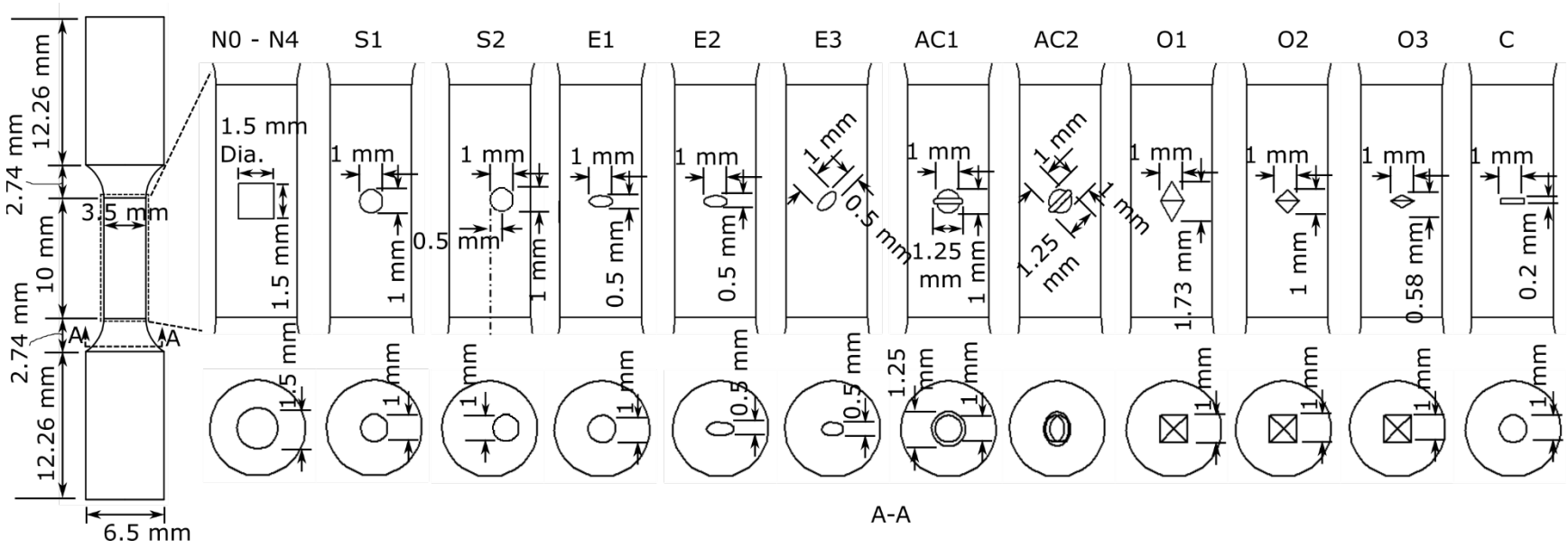

Fig. 7. Initial AM tensile specimen build geometry and geometry of embedded defects

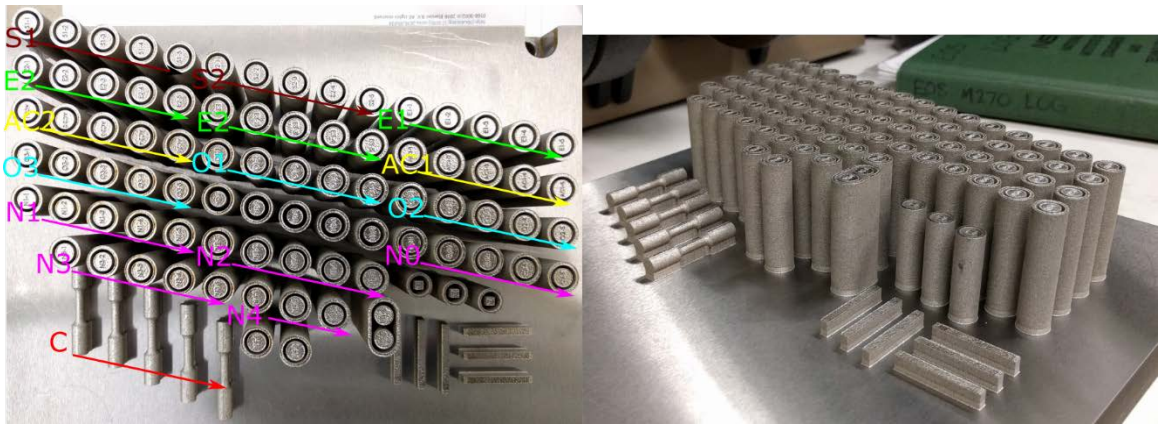

Fig. 8. Build plate of build 2

The build plate was heat treated at REX Heat Treat company to relieve residual stress before removing the specimens from the plate. The recommended heat treatment procedure for the material was to anneal at 650 °C (1202 °F) for 1 h followed by quenching in nitrogen [8]. The furnace temperature was ramped up within 2 h, and maintained at 650 °C ± 10 °C. A thermocouple was attached to a sample on the build plate to monitor the part temperature, and the heat treatment process started when the part temperature reached the annealing temperature.

After the heat treatment, a wire EDM was used to remove samples from the build plate. It is recommended to design the samples a little longer (e.g., 1 mm longer) to accommodate the EDM wire cut.

Due to the large number of specimens, a Computer Numeric Control (CNC) lathe was used for the machining. The support structure around the gauge section was first removed manually. The final shapes of the specimen with and without grooves are shown in Fig. 9a. The final shape without the grooves was produced with a CNC lathe successfully. The center gauge section of the specimen was first held by a brass split ring, which was held by a collet. Then, one of the grip sections was turned down to the major diameter. The specimen was flipped, and the process was repeated on the other grip section. Then, the grip area was held down by a collet, and a half of the gauge section was machined by using a 35° turning tool. The specimen was flipped, and the process was repeated for the other half of the gauge section. Machining the grooves using the CNC lathe was tried, but it turned out to be difficult to hold the small specimen at the thinner gauge section and control the machining process without damaging the specimen. Instead, a programmable manual lathe was used to machine the grooves, which took longer to finish. Center indents were produced at each end first to be used by the tail stock of the lathe. Then, the gauge section was held down by another brass split ring and a collet. The tail stock was used to support the other end of the specimen. A tool with a 90° tip was used to produce grooves on one side of the grip. Then, the specimen was flipped and the process was repeated on the other side. The final specimens after the machining process are shown in Fig. 9b, and the grooved specimen has a good fit with the grips as shown in Fig. 9c. In future builds, however, it is recommended to build the sample in cylinder shape (design 1). In this case, the machining sequence can be changed to machine

the grooves before machining the reduced gauge section, all of which can be performed on a CNC lathe machine to expedite the process.

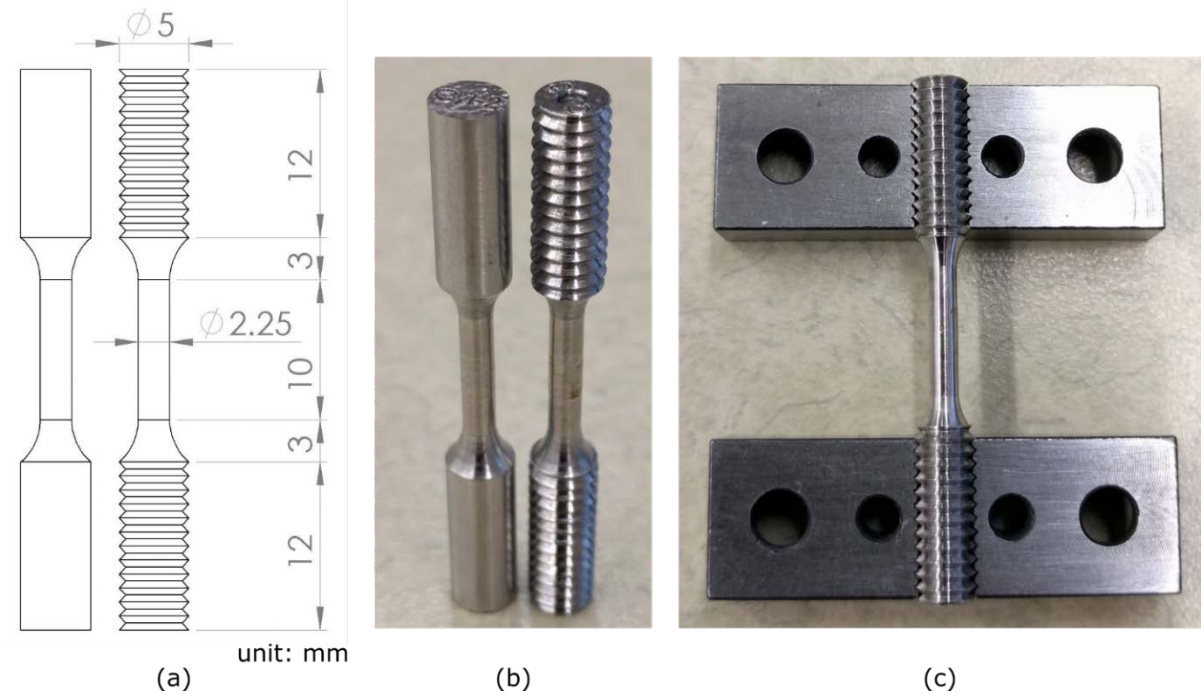

Fig. 9. (a) Designs of final shape, (b) picture of specimens after machining, and (c) a specimen fit to grips

6. Conclusions

A process to prepare a small cylindrical tensile specimen using AM and conventional machining was developed. The cylindrical tensile specimens were specifically developed to be tested in the loading system while XCT images were captured. Since the rough surfaces of the as-built AM may act as local stress concentrators, affecting the mechanical strength and failure mechanism, post process machining of critical surfaces is generally recommended. Therefore, it is important to consider the post process machining during the AM design phase. The post process machining was challenging partially due to the small size of the specimen, and a simpler initial AM geometry would have made the post-machining easier. Two different methods of embedding defects in the mechanical test specimens were tried, and the results will be revealed in the future XCT scans of the specimens. The first method was to change the AM processing parameters, and the second method was to design the defects. AM provides an opportunity to embed such defects at the location of interest, and this type of capability can be useful for research projects involving fracture mechanics. The dimensional XCT technique was also applied on the produced tensile specimen and received specimen grips for inspection of the machining quality. The XCT-based inspection technique can be useful for inspecting smaller parts that are difficult or time-consuming with alternative techniques. This paper can provide a guideline for developing smaller tensile specimens with AM.

References

[1] ASTM E8/E8M (2016) Standard Test Methods for Tension Testing of Metallic Materials. (ASTM International).

[2] EOS GmbH - Electro Optical Systems (2009) EOS StainlessSteel GP1 for EOSINT M 270.

[3] Berger MJ, Hubbell JH, Seltzer SM, Chang J, Coursey JS, Sukumar R, Zucker DS, Olsen K (1998) XCOM: Photon Cross Sections Database. *NIST Standard reference database 81*:3587-3597.

[4] VDI (2011) Computed Tomography in Dimensional Measurement-Guideline for the Application of DIN EN ISO 10360 for Coordinate Measuring Machines with CT-sensors VDI/VDE 2630-1.3. (Beuth Verlag GmbH, Berlin).

[5] Christof R (2008) Industrial computer tomography - a universal inspection tool. *17th World Conference on Nondestructive Testing*.

[6] Kim FH, Moylan SP, Garboczi EJ, Slotwinski JA (2017) Investigation of pore structure in cobalt chrome additively manufactured parts using X-ray computed tomography and three-dimensional image analysis. *Additive Manufacturing* 17:23-38. https://doi.org/http://dx.doi.org/10.1016/j.addma.2017.06.011

[7] Kim FH, Villarraga-Gómez H, Moylan SP (2016) Inspection of Embedded Internal Features in Additively Manufactured Metal Parts Using Metrological X-ray Computed Tomography. in *ASPE/euspen 2016 Summer Topical Meeting Dimensional Accuracy and Surface Finish in Additive Manufacturing* (American Society for Precision Engineering, Raleigh, NC), pp 191-195.

[8] Cheruvathur S, Lass EA, Campbell CE (2016) Additive Manufacturing of 17-4 PH Stainless Steel: Post-processing Heat Treatment to Achieve Uniform Reproducible Microstructure. *JOM* 68(3):930-942. https://doi.org/10.1007/s11837-015-1754-4